Physica Scripta. Vol. 57, 228–232, 1998

Coherent Phenomenon in Reflection of Radiation by an Uneven Mirror

N. Artemiev,* A. Artemiev, V. Kohn and N. Smolyakov

Russian Research Centre "Kurchatov Institute", 123182, Moscow, Russia

Received March 19, 1997; accepted April 1, 1997

PACS Ref: 42.10

Abstract

First experimental results are presented for a coherent phenomenon in reflection of radiation by a mirror with a concave round surface. It consists of interference fringes which arise owing to the interaction of rays undergoing different numbers of reflections on the mirror. An analytical theory of the phenomenon is given in the frame of a geometrical optics approach in a small angle approximation. The experimentally measured interference fringes for the visual light of a Ne–He laser reflected by the round part of the mirror are in qualitative coincidence with the results of accurate computer calculations performed in the frame of a geometrical optics approach.

1. Introduction

As it is well known, interference phenomena are observed with coherent radiation characterized by a well determined wavelength λ and direction of propagation [1]. Interference strips arise due to the difference in optical paths of an integer number of wavelengths between the interfering beams. In the simple case of plane wavefront beams this difference arises when the beams intersect each other in space under the definite angle $\Delta\theta$. The ray path difference is $\Delta r_{12} = \Delta\xi\ \Delta\theta$ where $\Delta\xi$ is the distance between two points on the fringes pattern. Therefore the distance between two neighboring strips (the period of intensity oscillations) equals $\Delta\xi_p = \lambda/\Delta\theta$. If the angle $\Delta\theta$ is small enough then the fringes can be seen directly even for small wavelengths. Each interference device has to have a splitter which divides one beam into two beams and a system of mirrors or other elements which deflect the direction of the beams to make them intersect each other.

The classic interference devices like the Fresnel biprism are usually symmetrical. These caused only the angle between beams while the absolute ray path difference in the central position equals zero. Such a device allows to observe interference fringes even under the condition of poor temporal coherence when the longitudinal coherence length exceeds only a few wavelengths. When the source has a high degree of temporal coherence like a laser or there is a possibility to monochromatize the incident beam as in high energy X-ray optics this condition is not necessary and one may consider the asymmetric interference device when different parts of the initial beam interfere directly. One of such devices is presented and studied both theoretically and experimentally in this paper. It is the reflection of a parallel beam by an uneven concave mirror under grazing incidence when one part of the beam can make one reflection, a second part – two reflections and so on. The rays which perform different numbers of reflections leave the surface under different angles [see Fig. 1(a)].

For example, with a laser light wavelength $\lambda = 0.63\,\mu$m and $\Delta\theta = 2$ mrad we obtain $\Delta\xi_p \approx 0.3$ mm. For X-rays with $\lambda = 10^{-4}\,\mu$m and $\Delta\theta = 0.01$ mrad we obtain $\Delta\xi_p \approx 10\,\mu$m. Thus we arrive to a conclusion that the interference fringes can be observable for both laser light and X-rays. However, the angle between interfering beams must have different orders of magnitude. Let r_{sd} be the distance between the reflecting area of the surface and the detector, θ_0 be the angle between the direction of the reflected beam and the "middle plane" of the surface. Then we can estimate the distance between different reflecting areas of the surface,

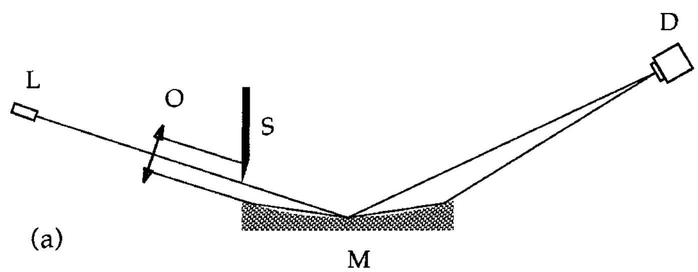

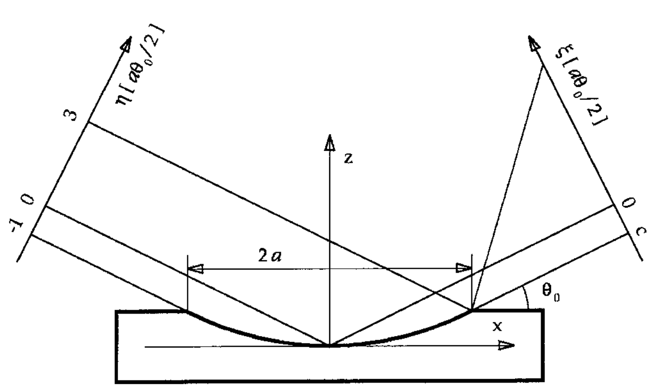

Fig. 1. (a) Experimental layout. L – Ne–He-laser, O – objective, S – slit with moving upper edge, M – cylindrical mirror, D – detector (CCD matrix), (b) Geometrical parameters of the theory. The point c is the centre of the interference pattern.

* E-mail: nikolai@ksrs.msk.su

$\Delta x \approx \Delta\theta r_{sd}/\theta_0$, while the distance between different parts of the incident beam which interfere is $\Delta\eta \approx r_{sd}\Delta\theta$. For example, for $\theta_0 \approx 100\ \Delta\theta$ we have $\Delta\eta = 2$ mm for laser light and $\Delta\eta = 10\ \mu$m for X-rays while $\Delta x = 1$ cm in both cases. The estimations performed allows to conclude that this kind of interference pattern is more easy to observe in a laser light. On the other hand, it can be used for testing a surface of mirror of extremely high quality with coherent X-rays owing to very high sensitivity of X-rays to this kind of interference.

The limiting case of multiple reflection of the beam by a concave mirror when the radiation propagates along the mirror surface are known (see, for example [2]). A practical implementation of the effect is being developed, the Kumakhov lens [3, 4]. However, the interference fringes described above were out of the study. Nevertheless we think it is of interest to understand the possibility of this technique to test the coherence property of a beam especially for synchrotron radiation after a monochromator system. To make ourselves sure about the result we have first performed the experiments with a laser source having a great degree of coherence.

2. Theory

To obtain a qualitative picture of the effect under consideration we shall use geometrical optics. In this approach at a first stage one has to draw a surface of constant phase of the incident radiation. For an incident plane wave it is a plane normal to the beam direction. A ray has a direction normal to a surface of constant phase at the point of its beginning. In empty space a ray trajectory is a straight line. After a reflection of a ray by an even fragment of a surface we have $E_1 = R_s E_0$ where the reflection amplitude R_s satisfies the same rule as the plane wave, namely, Fresnel formulas [1]. When the angle of incidence $\theta_0 \ll \sqrt{|\chi|}$ ($\chi = \varepsilon - 1$ is the susceptibility of the mirror matter) the reflection amplitude $R_s \approx -1$.

Let us consider the case where all reflections occur in one plane (the mirror has a cylindrical shape). Let η be a coordinate along the front of the incident plane wave while ξ be a coordinate along the detector line [see Fig. 1(b)]. The amplitude of the field which is brought by the ray having a beginning at η and the end at ξ is defined as

$$E(\eta) = \left(\frac{d\xi}{d\eta}\right)^{-1/2} R_t(\eta) \exp\left[\frac{2\pi i}{\lambda} r_t(\eta)\right], \quad \xi = \xi(\eta). \tag{1}$$

Here we assume that the incident wave has a homogeneous density of rays while at the detector the rays can have an inhomogeneous density which is measured by $(d\xi/d\eta)^{-1}$. In (1) $R_t(\eta)$ is the total reflection amplitude, $r_t(\eta)$ is the total ray path length from η to ξ. The functions $\xi(\eta)$, $r_t(\eta)$ and $R_t(\eta)$ are single defined that means, for example, one value of ξ for each value of η. Nevertheless, the function $\xi(\eta)$ may take the same value for different η. It means that the reverse function $\eta(\xi)$ may have a multiple branch structure $\eta_j(\xi)$. Therefore the real intensity at the point ξ is calculated as follows

$$I(\xi) = \left|\sum_{j=1}^{j_{\max}} E[\eta_j(\xi)]\right|^2. \tag{2}$$

Interference fringes are possible to observe in cases where $j_{\max} \geqslant 2$.

We shall consider a surface with a round pit of radius R which is very large compared to the size of the pit, $2a$ [Fig. 1(b)]. In this geometry all angles are small and we shall use a linear approximation to make formulas simpler and to obtain the result in an analytical form. A rectangular coordinate system (x, z) is shown in Fig. 1(b) as well. The equation of the surface is as follows $z = R - \sqrt{R^2 - x^2} \approx x^2/2R$. The slope of the surface at the point x can be characterized by an angle between a tangent line to the surface and the X-axis, $\theta_s = dz/dx = x/R$. The maximum slope corresponds to the end of the pit and equals $\theta_0 = a/R$.

Let the angle for an incident beam equal $-\theta_0$. The ray path within the incident beam is described in the linear approximation as $z = -\theta_0 x + \eta$ [see Fig. 1(b)]. The solution in common of this equation with the equation of the surface gives the x, z coordinates of the point of first reflection. It is enough to characterize this point by only the x-coordinate because the z-coordinate is defined by the equation of the surface. Thus we obtain

$$x_1 = a(s - 1), \quad s = \sqrt{1 + \frac{2\eta}{a\theta_0}}. \tag{3}$$

Here we introduce a new ray parameter s. It is evident that the value of s runs from 0 to 2. Therefore η has values from $-a\theta_0/2$ to $3a\theta_0/2$ [see Fig. 1(b)]. The index shows that this point is the point of first reflection. The angle of the reflected ray is defined by the general rule $\theta_{out} - \theta_s = \theta_s - \theta_{in}$, in our case $\theta_{out} = \theta_1$, $\theta_{in} = -\theta_0$, therefore we have $\theta_1 = 2\theta_s + \theta_0$ and taking into account that $\theta_s = x_1/R$ we obtain $\theta_1 = \theta_0(2s - 1)$. The trajectory of the ray will follow the perimeter of an inscribed polygon. Therefore, in following reflections the angle will change with the same value. This allows us to write directly for the n-th reflection

$$\theta_n = \theta_0(2ns - 1), \quad x_n = a([2n - 1]s - 1). \tag{4}$$

The number of possible reflections is determined from the condition that the point of the next reflection exceeds the size of the spherical pit a, therefore $s < s_{n\max} = 2/(2n - 1)$ for n reflections.

This means that one reflection occurs for $2/3 < s < 2$, two reflections occur for $2/5 < s < 2/3$, and so on. On the other hand, the equation $\eta = \frac{1}{2}a\theta_0(s^2 - 1)$ allows to define the boundary of zones in terms of the η-variable. It is convenient to use a dimensionless variable $\eta' = 2\eta/a\theta_0 = s^2 - 1$. Let r_{sd} be the distance from the centre of the mirror to the detector. Then the point of intersection of the outgoing ray with the detector line is $\xi(\eta, n) = r_{sd}(\theta_n - \theta_0) + z_n - \theta_n x_n$. Substituting the expressions for θ_n, x_n and $z_n = x_n^2/2R$ we obtain for the dimensionless variable:

$$\begin{aligned}\xi'(\eta, n) &= 2\xi/a\theta_0 = \\ &= 4r'_{sd}(sn - 1) - ([2n - 1]s - 1)([2n + 1]s - 1), \\ r'_{sd} &= r_{sd}/a.\end{aligned} \tag{5}$$

We are interested in the reverse dependence $s = s(\xi)$. The dependence may be multiple defined $s = s_n(\xi)$. Below we restrict ourselves only to the case where the distance between the mirror and the detector is very large $r'_{sd} \gg 1$ assuming simultaneously that ξ'/r'_{sd} can be significant. In this limit we shall obtain the solution as a power series expansion over $1/r'_{sd}$ up to the first order

$$s_n(\xi) \approx \left(\alpha + \frac{\alpha(\alpha-1)}{r'_{sd}}\right)\frac{1}{n} - \frac{\alpha^2}{4r'_{sd}}\frac{1}{n^3}, \quad \alpha = 1 + \frac{\xi'+1}{4r'_{sd}}, \tag{6}$$

while

$$\eta'_n = s_n^2 - 1, \quad I_n(\xi) = \left(\frac{d\xi}{d\eta}\right)^{-1}_{s=s_n(\xi)} \approx \frac{\alpha}{2n^2 r'_{sd}}. \tag{7}$$

The solution (6) allows to determine the main characteristic of interest, namely, the angle difference at positions of various beams which intersect at the same point at the detector [see Fig. 1(a)]. With the use of (4) one has

$$\Delta\theta_{nm} = \theta_n(\xi) - \theta_m(\xi) = \frac{\theta_0\alpha^2}{2r'_{sd}}\left(\frac{1}{m^2} - \frac{1}{n^2}\right). \tag{8}$$

Let us make an estimation for $r_{sd} = 100\,\mathrm{cm}$, $a = 3.2\,\mathrm{cm}$, $R = 20\,\mathrm{cm}$. Under these conditions we obtain $\theta_0 = 0.16$, $r'_{sd} = 31.2$. At the point $\xi = -a\theta_0/2 = \eta_{\min}$ we have $\xi' = -1$, $\alpha = 1$ and according to (6) $s_n = n^{-1} - 0.008n^{-3}$. The boundaries of the n-th band are defined by $s_{n\,\max} = 1/(n-1/2)$, $s_{n\,\min} = 1/(n+1/2)$. Therefore, the number of possible bands equals infinity i.e. together with the ray which glances along the surface as a result of infinite reflections there exist also rays which have made one, two, etc. reflections. The angles between different rays are different. Equation (8) gives the estimation $\Delta\theta_{21} = 0.012\theta_0 = 0.0019$, $\Delta\theta_{31} = \Delta\theta_{31}\frac{32}{27} = 0.0022$, $\Delta\theta_{32} = \Delta\theta_{31} - \Delta\theta_{21} = 0.0003$, etc. For laser light with $\lambda = 0.633\,\mu\mathrm{m}$ we obtain the main period of oscillations, $\Delta\xi_{21} \approx 0.3\,\mathrm{mm}$.

In another point, for example, $\xi' = -1 + 0.88r'_{sd}$ we obtain $s_n = 1.228n^{-1} - 0.012n^{-3}$. Now $x_3 = 1.05a$ and therefore only two reflections are possible. The angles $\Delta\theta_{nm}$ become larger because $\alpha^2 = 1.5$ while the period of oscillations $\Delta\xi_{21} \approx 0.2\,\mathrm{mm}$. The angle between rays depends on ξ rather slightly, therefore near some point pure sinusoidal oscillations will be observed with the same period.

The calculated parameters allows to estimate the intensity distribution inside any local region at the detector. Let us assume that the angles of reflection are small enough to neglect the angular dependence of the reflection amplitude and to take $R_t(\theta) \approx -1$. Then

$$I(\xi + \Delta\xi) = \sum_{n=1}^{n_{\max}}\left[I_n + 2\,\mathrm{Re}\sum_{m<n}(-1)^{n+m}(I_n I_m)^{1/2} \times \exp\left(\frac{2\pi i}{\lambda}[r_{nm} + \Delta\theta_{nm}\Delta\xi]\right)\right]. \tag{9}$$

Here $n_{\max}$ is the total number of rays possible for a given point ξ, I_n and $\Delta\theta_{nm}$ are defined by (7), (8) while $r_{nm}(\xi) = r_n(\xi) - r_m(\xi)$ is the absolute ray path difference where $r_n(\xi)$ is the total ray path length from the origin to the point ξ at the detector for the n-th band. In calculating the $\Delta\xi$ dependence one can keep the values $r_{nm}(\xi)$ constant. This influences the interference pattern very slightly for a completely coherent radiation.

Let us consider now a case of finite longitudinal (temporal) coherence. In this case the observed intensity must be averaged over the spectral width of the radiation. Let the function $S(\lambda_1)$ describe the spectral distribution of incident radiation near the wavelength λ. We shall assume this function to be a normalized Gaussian distribution of width σ, namely, $S(\lambda_1) = 2(\sigma\sqrt{\pi})^{-1}\exp(-4\lambda_1^2\sigma^{-2})$. Then assuming $\lambda_1 \ll \lambda$ we represent the factor $\exp[2\pi i r_{nm}/(\lambda+\lambda_1)]$ as $\exp(2\pi i r_{nm}/\lambda)\exp(-2\pi i r_{nm}\lambda_1/\lambda^2)$ and calculate the average value of the second exponential

$$C_{nm}(\xi) = \int_{-\infty}^{\infty} d\lambda_1 \exp\left(-\frac{2\pi i}{\lambda^2}r_{nm}(\xi)\lambda_1\right)S(\lambda_1) = \exp\left(-\frac{\pi}{4}\left[\frac{r_{nm}(\xi)}{\lambda^2}\sigma\right]^2\right). \tag{10}$$

As a result the expression (9) takes the form

$$I(\xi + \Delta\xi) = \sum_{n=1}^{n_{\max}}\left[I_n + 2\,\mathrm{Re}\sum_{m<n}(-1)^{n+m}(I_n I_m)^{1/2}C_{nm} \times \exp\left(\frac{2\pi i}{\lambda}[r_{nm} + \Delta\theta_{nm}\Delta\xi]\right)\right]. \tag{11}$$

One can see that the wide spectral width of the incident radiation leads to decreasing interference fringes similarly to the Debye–Waller factors in X-ray Bragg diffraction. It is easy to estimate the temporal coherence needed for observation of the interference fringes. The bandwidth of the radiation, σ, has to satisfy the condition

$$\sigma \ll \frac{\lambda^2}{r_{21}(\xi)}. \tag{12}$$

To use this equation we have to calculate the value $r_{21}(\xi)$ with better accuracy than considered above. This may be performed with the result

$$r_n = r_0 + r_{sd} + \frac{1}{2}r_{sd}(\theta_n^2 - \theta_0^2) - (\eta + \xi)\theta_0 - \frac{1}{2}\sum_{m=1}^{n} x_m(\theta_m^2 - \theta_{m-1}^2). \tag{13}$$

Substituting (4) and (6) and conserving only the main terms we arrive at the expression

$$r_n = C + a\theta_0^2\left(\frac{A_n}{n^2} - \frac{B_n}{n^3}\right) \tag{14}$$

where C does not depend on n while

$$A_n = \alpha^2\left[4\sum_{m=1}^{n}(2m-1) - \alpha\right], \quad B_n = 2\alpha^3\sum_{m=1}^{n}(2m-1)^2. \tag{15}$$

For example, if $\alpha = 1$ ($\xi' = -1$) then $r_{21} \approx \frac{1}{4}a\theta_0^2$. For the condition considered above ($\theta_0 = 0.16$, $a = 3.2\,\mathrm{cm}$), we obtain the estimation $r_{21} \approx 0.02\,\mathrm{cm}$. This leads to a degree of light monochromaticity $\Delta\lambda/\lambda = \lambda/r_{21} \approx 3.2 \cdot 10^{-3}$ for $\lambda = 0.633\,\mu m$ ($\sigma = 2\,\mathrm{nm}$) which is quite reachable for laser light. On the other hand one can see that the ray path difference contains about 300 wavelength.

The derived formulas allow to draw a conclusion about the general properties of the interference pattern. As it follows from (6) the parameter α increases slightly with increasing ξ. In accordance with (8) and (9) we may conclude that the period of oscillations will decrease and the amplitude of oscillations will increase with increasing ξ. Possible values of α for different bands follow from (6).

Approximately, the area for a path with n reflections is as follows

$$\frac{1}{1+1/2n} < \alpha < \frac{1}{1-1/2n}. \tag{16}$$

This formula shows that areas for different reflections coincide very well as there exists a possibility of interference of many different rays with different numbers of reflections from 1 to infinity. However, the more number of rays interfere the narrower becomes the region with the centre at $\alpha = 1$ ($\xi' = -1$).

3. Experiment and discussion

The experimental layout is given in Fig. 1(a). A Ne–He laser ($\lambda = 0.633\,\mu$m) and an objective ($f = 100$ m) give practically a plane wave of radiation. We use a cylindrical mirror with 20 cm radius while the central angle of reflection is 0.32 rad. A slit is placed directly before the mirror. The lower edge of the slit always coincides with the front edge of the concave region of the mirror while the upper edge can move in vertical direction to change the input aperture of the laser beam. By means of fine rotation we have the possibility to set the tangent to the front edge of the cylindrical shape parallel to the beam axis. The size of the beam is three times more than that of the input slit. Therefore we have a practically constant beam intensity in vertical direction in the limits of the input slit. However we can change the beam size moving up or down the upper edge of the input slit. By means of adding gray filters we can adjust the intensity on the screen to use the full dynamical range of the detector.

A CCD matrix without any objective is used as a detector (5.5×7 mm matrix size, 336×288 resolution). The matrix plane is perpendicular to the tangent of the rear edge of the cylindrical region of the mirror. The distance between the mirror and the matrix plane is 1 m. We have the opportunity to put the detector at any place of the interference picture. The matrix accumulation time was 320 ms. When switching off the laser beam we measure a background intensity which is about 2–3% of the full detector dynamic range.

First of all let us give a general picture of the phenomenon observed. When a simple screen is put behind the mirror we easily see a rather complicated picture which contains parts with a constant gray level and parts with interference structures of different kind. If the full concave region of the mirror is irradiated (the height of the vertical aperture is 10.24 mm) the length of the whole picture on the screen is 420 mm. When the input vertical aperture is decreased by the top edge of the slit the interference picture on the screen changes in a rather complex way.

For the first detailed investigation we choose the simpler part of the picture and use the CCD matrix instead of the screen to get the best resolution as is shown in Fig. 1(a). Figure 2 shows raw experimental data while Fig. 3 shows the same experimental data in numerical form after computer processing. Figures 2 and 3 show three different parts of the total picture corresponding to the interference of the rays which perform one and two reflections (a); one, two and three reflections (b); two and three reflections when the ray of one reflection cannot pass through the slit (c).

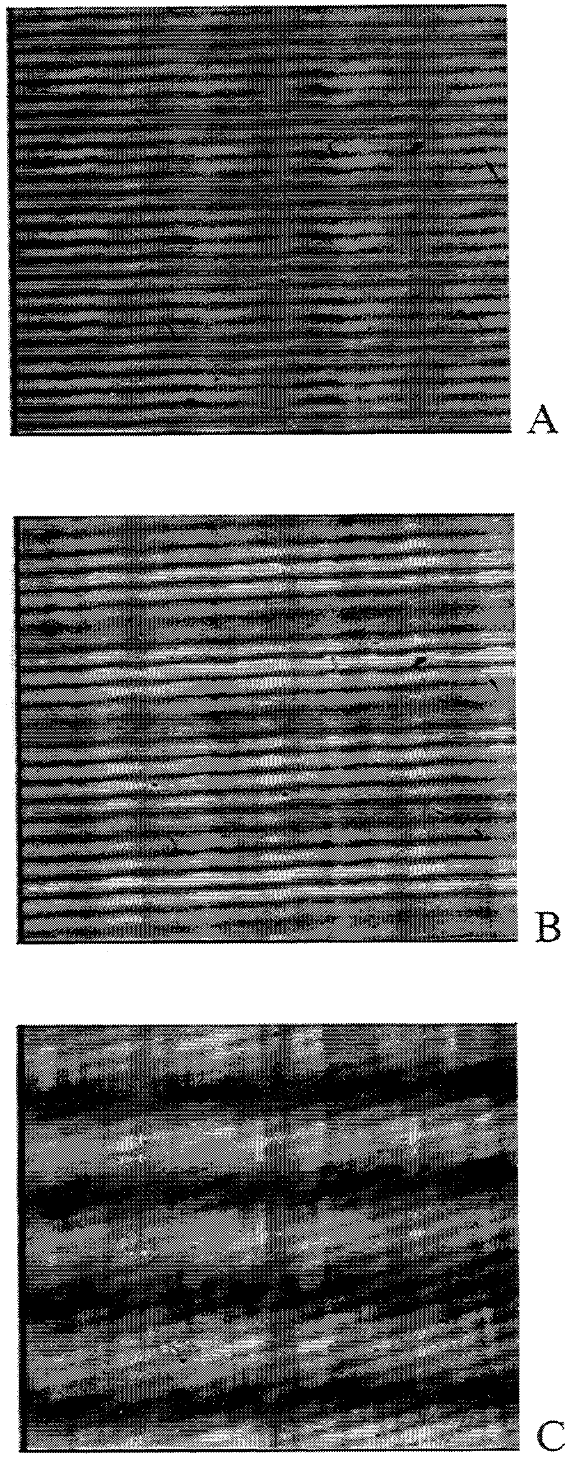

Fig. 2. Raw experimental data. The change of data along the axis of the cylindrical mirror is due to an inhomogeneous beam and other reasons (see text). A, B and C pictures correspond to Fig. 3 (see title).

The vertical direction of Fig. 2 practically coincides with the ξ-axis in Fig. 1(b) while the horizontal direction of Fig. 2 is perpendicular to the scattering plane (shown in Fig. 1). One can see a periodical change of the gray level in vertical direction sometimes of different amplitude. To obtain numerical data from these pictures we use the following procedure. The digital intensity measured by the pixels having a position strictly along the interference strip has been summarized. As it was mentioned before these interference strips have almost horizontal direction in Fig. 2. Therefore, any inhomogeneity in the registration by different pixels, the inhomogeneity of the input radiation and the inhomoge-

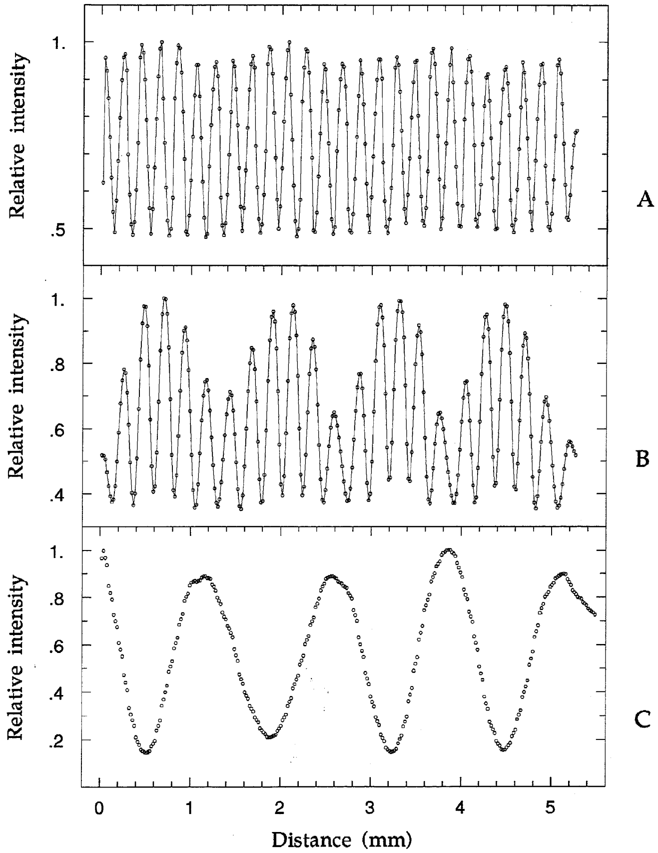

Fig. 3. Experimental interference pattern under different conditions: A – the waves after 1 and 2 reflections interfere, B – the waves after 1, 2 and 3 reflections interfere, C – the waves after 2 and 3 reflections interfere while the wave after 1 reflection is cut off by a slit.

neity of the mirror surface become of less importance. All these inhomogeneities can easily be seen in the raw data as the aperiodic blackening changes in the horizontal direction in Fig. 2. All summarized data were normalized to unity. We do not eliminate the background and the noise from the raw experimental data.

The experimental points are shown in Fig. 3 by circles which are connected by straight segments to have a better view of the dependence. Figure 3(a) gives the intensity distribution measured on the place of the screen where two rays interfere after one and two reflections, correspondingly. The period of oscillations in vertical direction is about $\Delta\xi_{12} = 0.2$ mm. Figure 3(b) gives the intensity distribution measured inside the region where three rays interfere after one, two and three reflections, correspondingly. The periodic structure with the period $\Delta\xi_{12} = 0.2$ mm remains but there exists an additional modulation with a period $\Delta\xi_{23} = 1.3$ mm. Figure 3(c) shows the intensity distribution measured at the region where two rays interfere after two and three reflections, correspondingly, while the ray undergoing one reflection is cut off by a slit. Here the periodical structure of the period $\Delta\xi_{12} = 0.2$ mm disappears and only the structure of the period $\Delta\xi_{23} = 1.3$ mm is clearly visible. Figures 3(b) and 3(c) correspond approximately the same region but to remove rays of the first zone we simply move down the upper edge of the slit from 10.24 to 1.15 mm.

We have performed theoretical calculations in the frame of a geometrical optics approach for the specific parameters of the experiment. We did not use the small angle approximation of the analytical theory presented above. We have found a qualitative coincidence of the results of calculations with the predictions of analytical theory as well as with the experimental results obtained. This paper is devoted only to the presentation of the idea and first experimental results. We do not perform a complete analysis of fine disagreements. The qualitative coincidence of experimental and calculated results allows to conclude that the main peculiarities of the phenomenon are described well enough in the frame of the geometrical optics approach. Nevertheless, it is of interest to discuss some discords.

One can see that the experimental sine curve in Fig. 3(a) is slightly modulated. The same occurs in Fig. 3(c). As for Fig. 3(b) we want to notice that the relation of short and long periods, $\Delta\xi_{12}/\Delta\xi_{23}$, of oscillations in the experimental curve becomes slightly different compared to the calculated value. In addition, some new peculiarities of the intensity behaviour in the boundary region between two neighbour zones were observed. We think that the main reason for this disagreement is the possible diffraction phenomena which arise for long distances between the mirror and the detector (in our case it was 1 m). These diffraction phenomena can be evaluated theoretically in the frame of the Fresnel–Kirchhoff approach. We plan to perform this detailed analysis in further work.

In conclusion, we note that the coherent phenomenon considered here may be useful for an investigation of the source characteristics (for example, for a synchrotron radiation source) as well as shapes and surface roughnesses of mirrors.

Acknowledgement

Authors express great gratitude to O. Chubar for the CCD detector with primary software and A. D. Kharitonov for help.

References

1. Born, M. and Wolf, E., "Principles of Optics" (Pergamon Press, Oxford 1968), 4th edn.
2. Vinogradov, A. V., Kovalev, V. F., Kozhevnikov, I. V. and Pustovalov, V. V., Zhurn. Techn. Fiz. **55**, 567 (1985).
3. Kumakhov, M. A. and Sharov, V. A., Nature (London) **357**, 390 (1992).
4. Dabagov, S. B. *et al.*, J. Synchrotron Rad. **2**, 132 (1995).